Development of 3,5–diiodobenzoic acid-based Halogen bond mediated Barrel Rosette Anion Channel

5th year MS thesis (August 2024)

By

Kavan Nandaniya

(Registration No. 20201167)

Under the Guidance of

Prof. Pinaki Talukdar

Department of Chemistry

Indian Institute of Science Education and Research Pune

Dr.Homi Bhabha Road, Pashan, Pune

Certificate

This is to certify that this dissertation entitled “Development of 3,5–diiodobenzoicacid-based Halogen bond mediated Barrel Rosette Anion Channel” towards the partial fulfillment of the BS-MS dual degree programme at the Indian Institute of Science Education and Research, Pune represents study/work carried out by Kavan Nandaniya at the Indian Institute of Science Education and Research (IISER) Pune, under the supervision of Prof. Pinaki Talukdar, Department of chemistry IISER, Pune during the academic year 2024-2025.

Signature of Supervisor

Declaration

I hereby declare that the matter embodied in the report entitled “Development of 3,5–diiodobenzoicacid-based Halogen bond mediated Barrel Rosette Anion Channel” are the results of the work carried out by me at the Department of Chemistry, Indian Institute of Science Education and Research (IISER) Pune, under the supervision of Prof. Pinaki Talukdar, and the same has not been submitted elsewhere for any other degree.

Kavan Nandaniya

20201167

Signature of student

Acknowledgments

I would like to express my thanks to my thesis supervisor, Prof. Pinaki Talukdar, for the opportunity to work in his lab a year prior to starting my MS thesis. I am truly appreciative of his guidance, encouragement, and unwavering support throughout my journey.

I would like to thank Prof. M. Jayakannan (IISER, Pune) for accepting to be my expert for the MS-thesis work and for the valuable inputs during my Mid-term report

I would like to thank Dr. Sandip Chattopadhayay, whose constant guidance and support made the challenging learning experience very easy. I have been blessed with a group of people who have supported me throughout the project. I thank Akram Raza, Dr. Avisikta Upadhyay, Debarati Sadhukhan, Debraj Ganguly, Neelam Raturi, Pathan Shaharukh Khan, Payel Nandi, Dr. Rashmi Sharma, Ranjeet Patil, Soumayajit Ghosh, Tanvi Vyas, Ronedy Naorem, Ahan Chatterjee, Arshad A, Anirban Mukherjee, Shreya Das, Mayur Vadakte and Arjab Ray who are the past and present member of our lab for giving me all the supports and so many sweet memories during my project period.

My heartfelt thanks extend to my group friends, who have been an essential part of my journey throughout my master's program Divya, Pratiksha, Vishakha, Paritosh, Sachin, Nandeesh, Yashraj, Shresth Raj, Ansh, Ridham, Ayush, Rafael, Prince, Prashant, Dharmesh, Priyanshu, Karan, Somanko for their support outside the lab.

I am deeply thankful to my family for their love, patience, and encouragement; without them, I would not be able to reach this stage of my life.

Contents

Abbreviations

AMPA – alpha-amino-3-hydroxy-5-methyl-4-isoxazolepropionic acid

$CDCl_3$ – Chloroform-D

DIPEA – N,N-Diisopropylethylamine

DMF – Dimethylformamide

EYPC – Egg yolk phosphatidylcholine

FESEM – Field emission scanning electron microscope

HCl – Hydrogen chloride

HEPES – 4-(2-hydroxyethyl)-1-piperazineethanesulfonic acid

HPTS – 8-hydroxypyrene-1,3,6-trisulfonic acid

HRMS – High-resolution mass spectrometry

KI – Potassium iodide

LUVs – Larger unilamellar vesicles

$NaNO_2$ – Sodium nitrite

$NaNO_3$ – Sodium nitrate

NMR – Nuclear magnetic resonance

PMA – Phosphomolybdic Acid

rpm – Revolutions per minute

rt – Room temperature

$SOCl_2$ – Thionyl chloride

THF – Tetrahydrofuran

TLC – Thin-layer chromatography

1. Abstract:

Nature endowed different structurally and functionally complex transmembrane proteins that adequately maintain ionic homeostasis, which is essential for maintaining different physiological functions with an intention of understanding the ion transport process and making alternative synthetic analogous. Herein, we utilized 3,5-diiodo benzamide-based small molecules **1a**–**1d** which can assemble to form an ion channel in the membrane. Ion transport screening divulged that compound **1c** showed higher transport activity across the membrane. Self-assembly studies confirmed that compound **1c** has self-assembly properties. Detailed ion transport studies revealed that the compound can selectively transport the anions with preferential selectivity towards the chloride anion and it follows the antiport mechanism. The crystal structure of the compounds confirmed that the iodide atom has the tendency to form halogen bonding.

2. Introduction:

Accurate concentration of ions in living systems are maintained by membrane-embedded proteins in order to maintain the proper function of the cells. Natural protein channels like aquaporins and alpha-amino-3-hydroxy-5-methyl-4-isoxazolepropionic acid (AMPA) receptors are some examples of natural ion transporters. Learning from nature to construct such biomimetic ion channels is always challenging. In living systems, ion transport is essential for regulating the physiological pH level of some tissues or organelles to facilitate physiological functions, which are usually mediated by specific protein channels.[1] Chloride, the primary extracellular anion, plays a vital role in regulating osmotic balance and pH stability in bodily fluids, maintaining the cell volume, etc.[2,3] Its movement across cell membranes is mediated by specialized chloride channels, which are critical for establishing the resting membrane potential and influencing electrical excitability in neurons and muscles.[4–6] These channels also contribute to cellular processes like volume regulation, ion transport, and acid-base homeostasis.

Dysfunction in chloride transporters is linked to several genetic disorders, including Thomsen's disease (characterized by muscle stiffness), Dent's disease (kidney dysfunction), and Bartter's syndrome (electrolyte imbalance), etc.[7–9] Imbalances in chloride levels are associated with conditions such as metabolic alkalosis and renal tubular acidosis, often stemming from disrupted ion transport mechanisms in the kidneys or other tissues.[10,11] For example, mutations in chloride channels or their regulatory proteins can impair acid secretion in the stomach or chloride reabsorption in the kidneys, leading to systemic complications. Hence the regulation of chloride ion transporters exhibits promising therapeutic potential.[12–14] There are several reports where people have reported the synthetic ion channel which transports the ions through noncovalent interaction, hydrogen bonding, anion-π interaction, etc. The arrangement of small molecules in the lipid bilayer can create a more complex environment, which may impose a different geometry on the path that ions take across the bilayer. This affects the transport rate and selectivity of ions; so, to overcome this, halogen bond interactions play a crucial role, which helps to get a better transport rate and selectivity of ions by making it in lipophilic nature and increasing the cell permeability. Here, we are trying to design a 3,5-diiodo benzamide-based synthetic ion transporter that selectively transports the chloride ions across the lipid bilayer. The

objective of this project is to: (i) synthesize and characterize the different derivatives, (ii) compare ion transport activities and investigate the ion selectivity, (iii) investigate the operated ion transport mechanism by the synthetic transporter, (iv) reveal the mode (ion carrier or ion channel) of ion transport involved by the transporter molecule.

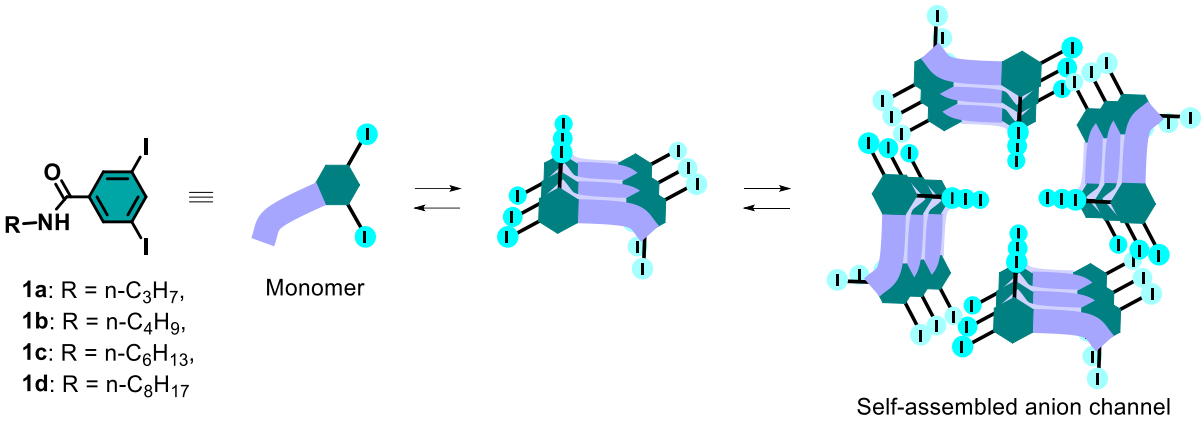

1a: R = n-C_3H_7,
1b: R = n-C_4H_9,
1c: R = n-C_6H_{13},
1d: R = n-C_8H_{17}

Figure 1: Structure of the channel forming compounds **1a**–**1d** and the probable formation of the self-assembled anion channel in the membrane.

3. General Methods and Results:

3.1. Materials used

For the synthesis and purification of all compounds in this thesis work, reagents, solvents, and starting materials were procured from commercial suppliers (Sigma-Aldrich, Hyma Synthesis, BLD Pharm, Spectrochem, TCI,) and used without further purification. Reactions were conducted under a nitrogen atmosphere using an N_2 gas balloon. Reaction progress and completion were monitored via thin-layer chromatography (TLC), with visualization under short-wave UV light or staining reagents such as Ninhydrin and PMA. Purification was performed using column chromatography with distilled organic solvents and silica gel (mesh size 100–200) from Sisco Chem. Egg yolk phosphatidylcholine (EYPC) was obtained as a 25 mg/mL solution in $CHCl_3$ from Avanti Polar Lipids. HEPES buffer, HPTS, Lucigenin, Triton X−100, NaOH, and inorganic salts (molecular biology grade) were sourced from Sigma. Larger unilamellar vesicles (LUVs) were prepared using a mini extruder (Avanti Polar Lipids) fitted with 100 nm or 200 nm pore-size polycarbonate membranes.

3.2. Physical Measurement

All ^{1}H and ^{13}C NMR spectra were recorded either on Bruker 400 MHz or Bruker 400 neo MHz spectrometers. The chemical shifts (δ) in ppm were referenced to the residual signal of deuterium solvents (^{1}H NMR $CDCl_3$: δ 7.26 ppm; ^{13}C NMR $CDCl_3$: δ 77.2 ppm) The multiplicities of the peaks are s (singlet), d (doublet), t (triplet), q (quartet), dd (doublet of doublet), and m (multiplet). High-resolution mass spectra (HRMS) were acquired in the ESI (+ve) mode. A pH meter was purchased from Thermo Scientific to measure the pH during the preparation of the buffer solution. Fluorescence spectra were recorded on a Fluoromax−4 from Horiba Scientific, Jobin Yvon Edison, equipped with an injector port and a magnetic stirrer. The field emission scanning electron microscopy (FESEM) images were obtained using FEI Quanta 3D dual beam ESEM at 3.0 kV. The experimental data obtained from fluorescence were processed in Origin 8.5 software. All figures and the chemical structures were drawn using ChemDraw 21.0.0.

3.3. Synthesis:

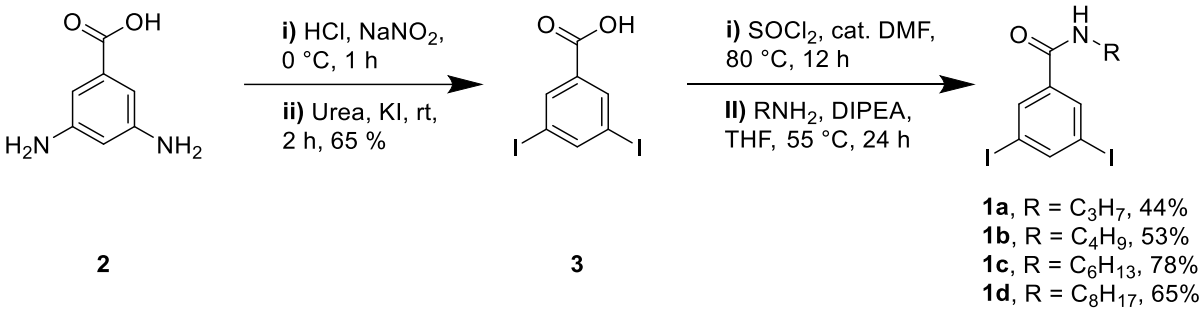

2 **3**

Scheme 1: The synthetic scheme for the synthesis of compound **1a**–**1d**.

Synthesis of compound 3: Compound **3** was synthesized following a known protocol.[15] At 0 °C, 5-amino isophthalic acid (3.0 g, 20 mmol) in a HCl solution was added to an aqueous solution of $NaNO_2$ (2.5 M). Afterward, urea (3.0 g) and KI (7.0 g) were added to the reaction mixture. The mixture was stirred for two hours. Following the addition of ice-cold water, the solid was filtered to get 3,5-diiodobenzoic acid (4.79 g, 65% Yield). ^{1}H NMR spectrum matched the data of the reported compound.[15]

The general synthetic procedure for the compound 1a–1d

In a clean and dry 25 mL round-bottomed flask, compound **3** (300 mg,1.10 mmol,1 equiv) was dissolved in $SOCl_2$ (4 mL), and a catalytic amount of DMF (2–3 drops) was

added to it. The reaction mixture was kept at 80 °C for 12 h. After the formation of the corresponding acid chloride of compound **3**, additional $SOCl_2$ was removed under reduced pressure, and the mixture was kept in a high vacuum for 30 min to remove the trace amount of $SOCl_2$ from it. The acid chloride was directly used for the next step reaction without further purification.

In another 25 mL round bottom flask, different alkyl amines (611.18 µmol,1.2 equiv.) were dissolved in dry THF (3 mL). After the addition of the required amount of DIPEA (329 mg, 2.55 mmol, 5 equiv), the reaction mixture was placed for stirring for about 15-20 minutes. The acid chloride (dissolved in 2 mL of THF) was added dropwise into the reaction mixture. After the complete addition of acid chloride, the reaction mixture was kept for stirring at 80 °C for 12 h. After completion of the reaction, THF and DIPEA were evaporated by using rota-evaporation. After transferring the mixture to a separating funnel with ethyl acetate (25 mL), it was washed with water (25 mL). The aqueous layer was then extracted three times with EtOAc (3×25 mL), and the combined organic layer was subsequently washed with a brine solution (25 mL). Next, Na_2SO_4 was used to dry the organic layer, and the solvent was evaporated under a rotary evaporator. Finally, purification of the crude product was performed using 100-200 mesh silica gel column chromatography.

Synthesis of 3,5-diiodo-N-propylbenzamide (1a): By taking 200 mg of compound **3**, compound **1a** was synthesized. The crude product was purified through column chromatography (Eluent: 4% ethyl acetate in petroleum) to obtain compound **1a** (93 mg). **Physical appearance:** Light yellow powder, **Yield** = 44%.**^{1}H NMR (401 MHz, $CDCl_3$):** δ 8.15 (t, *J* = 1.5 Hz, 1H), 8.01 (d, *J* = 1.5 Hz, 2H), 6.12 (s, 1H), 3.39 (q, *J* = 8.0, 7.2, 5.9 Hz, 2H), 1.68 – 1.58 (m, 4H), 0.98 (t, *J* = 7.4 Hz, 4H). **^{13}C NMR (101 MHz, $CDCl_3$):** δ 164.68, 147.83, 138.36, 135.36, 94.95, 42.17, 22.96, 11.58. **HRMS (ESI–MS) m/z:** $[M+H]^+$ Calcd. for $C_{10}H_{11}I_2NOH^+$ 415.9008; Found 415.9025.

Synthesis of N-butyl-3,5-diiodobenzamide (1b): By taking 200 mg of compound **3**, compound **1b** was synthesized. The crude product was purified through column chromatography (Eluent: 8% ethyl acetate in petroleum) to obtain compound **1b** (115 mg). **Physical appearance:** White powder, **Yield** = 53%. **^{1}H NMR (401 MHz,**

$CDCl_3$): δ 8.16 (t, *J* = 1.5 Hz, 1H), 8.01 (d, *J* = 1.5 Hz, 2H), 6.00 (s, 1H), 3.43 (dt, *J* = 7.2, 5.7 Hz, 2H), 1.65 – 1.56 (m, 9H), 1.47 – 1.34 (m, 2H), 0.96 (t, *J* = 7.3 Hz, 3H). **^{13}C NMR (101 MHz, $CDCl_3$):** δ 164.95, 148.15, 138.69, 135.67, 95.27, 40.54, 32.07, 20.59, 14.22. **HRMS (ESI–MS) m/z:** $[M+H]^+$ Calcd. for $C_{11}H_{13}I_2NOH^+$ 429.9165, Found 429.9165.

Synthesis of N-hexyl-3,5-diiodobenzamide (1c): By taking 200 mg of compound **3**,

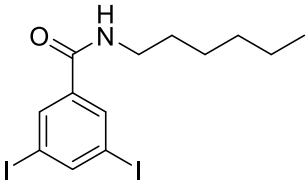

compound **1c** was synthesized. The crude product was purified through column chromatography (Eluent: 10% ethyl acetate in petroleum) to obtain compound **1c** (181 mg). **Physical appearance:** Light yellowish powder, **Yield** = 78%. **^{1}H NMR (400 MHz, $CDCl_3$):** δ 8.16 (t, J = 1.6 Hz, 1H), 8.02 (d, J = 1.5 Hz, 2H), 5.99 (s, 1H), 3.45 – 3.39 (m, 2H), 1.61 (p, J = 14.8, 7.7 Hz, 2H), 1.39 – 1.35 (m, 2H), 1.34 – 1.31 (m, 4H), 0.89 (t, 3H). **^{13}C NMR (101 MHz, $CDCl_3$):** δ 164.59, 147.85, 138.39, 135.35, 94.96, 40.54, 31.61, 29.68, 26.78, 22.69, 14.17. **HRMS (ESI–MS) m/z:** $[M+H]^+$ Calcd. for $C_{13}H_{17}I_2NOH^+$ 457.9472, Found 457.9486.

Synthesis of 3,5-diiodo-N-octylbenzamide (1d): By taking 200 mg of compound **3**,

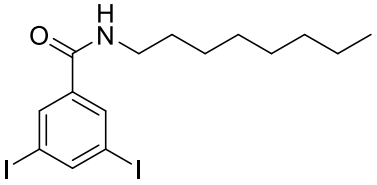

compound **1d** was synthesized. The crude product was purified through column chromatography (Eluent: 10% ethyl acetate in petroleum) to obtain compound **1d** (160 mg). **Physical appearance:** White powder, **Yield** = 65%. **^{1}H NMR (401 MHz, $CDCl_3$):** δ 8.16 (d, *J* = 1.4 Hz, 1H), 8.02 (t, *J* = 1.3 Hz, 2H), 5.97 (s, 1H), 3.42 (q, *J* = 6.7 Hz, 2H), 1.63 – 1.58 (m, 2H), 1.39 – 1.32 (m, 4H), 1.31 – 1.26 (m, 6H), 0.88 (t, 3H). **^{13}C NMR (101 MHz, $CDCl_3$):** δ 164.44, 147.72, 138.26, 135.21, 94.82, 40.40, 31.80, 29.57, 29.25, 29.18, 26.96, 22.65, 14.10. **HRMS (ESI–MS) m/z:** $[M+H]^+$ Calcd. for $C_{15}H_{21}I_2NOH^+$ 485.9791, Found 485.9792.

4. Results

4.1. Morphological study:

To understand the morphology of compound **1c**, Field emission scanning electron microscopy (FESEM) was performed. A 0.5 mM of compound **1c** was dissolved in HPLC grade MeOH, CH3CN, CH_3Cl and drop-casted (5 µL) on silicon wafers, and the

sample were dried over a high vacuum for 2 h. The elongated, rod-shaped images confirm the remarkably strong self-assembly of compound **1c**.

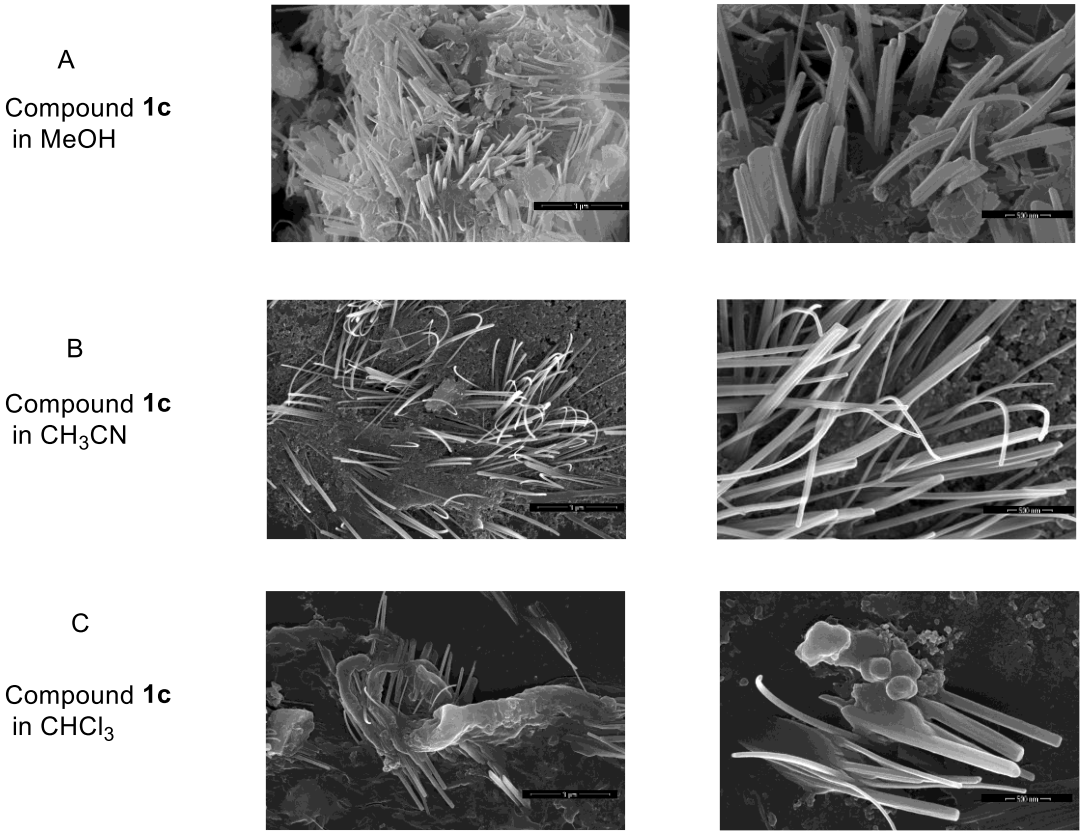

Figure 2: FESEM images of compound **1c** in different solvents: MeOH (A), CH_3CN (B), CH_3Cl (C) and all of them were recorded at 3 μm and 500 nm.

4.2. Ion Transport Studies:

4.2.1. Studies of ion transporting activity across EYPC-LUVs⊃HPTS:

Preparation of HEPES buffer and stock solutions: A 10 mM HEPES-based solution (pH 7.0) was formulated by dissolving stoichiometrically calculated quantities of HEPES powder (238.3 g/mol) and sodium chloride (58.44 g/mol) in sterilized deionized H_2O to achieve final concentrations of 10 mM and 100 mM, respectively. The pH was adjusted to 7.0 by adding aliquots from the NaOH solution (0.5 M). HPLC grade DMSO was used to prepare the stock solution for all the derivatives.[16–18]

Preparation of EYPC-LUVs⊃HPTS with NaCl: In a dry and clean round bottom flux (10 mL), 1 mL of egg yolk phosphatidylcholine (EYPC, 25 mg/mL in $CHCl_3$) was dried

by purging nitrogen gas with continuous rotation to make a thin transparent film of EYPC. Then, to remove a trace amount of $CHCl_3$, it was kept under a high vacuum for 4 h. Further, the dried thin film was hydrated with 1 mL HEPES buffer (1 mM HPTS, 10 mM HEPES, 100 mM NaCl, pH = 7.0), and the resulting suspension was vortexed for 1 h at 10 min intervals. The hydrated suspension underwent 23 cycles of freeze-thaw using liquid nitrogen and 55 °C hot water bath, followed by extrusion through a polycarbonate membrane with 0.1 μm pore size 23 times (ensuring an odd number cycles) to achieve a uniform distribution of LUVs with an average diameter of 100 nm. Next, size exclusion chromatography was performed using gel filtration with Sephadex G-50 to remove unentrapped extravesicular HPTS dyes using 4-(2-hydroxyethyl)-1-piperazineethanesulfonic acid buffer. The collected vesicles were then diluted to 6 mL to obtain EYPC-LUVs⊃HPTS. "Final conditions: ~ 5.0 mM EYPC, Outside: 10 mM HEPES, 100 mM NaCl, pH = 7.0, Inside: 1 mM HPTS, 10 mM HEPES, 100 mM NaCl, pH = 7.0."

Ion transport activity by HPTS assay: The HPTS assay is a fluorescence-based technique that for assessment of the ion transport process across the bilayer membranes utilizing synthetic molecules. It relies on the pH-sensitive dye HPTS (8-hydroxy-1,3,6-pyrenetrisulfonic acid) encapsulating inside the vesicles. In the presence of the synthetic ion channels or ion carrier, the movement of ions causes a change in the intravesicular pH, which can be detected through the changes in fluorescence emission intensity. This allows real-time tracking and quantification of the ion transport activity of synthesized compounds, making it helpful in studying various ion transport systems.

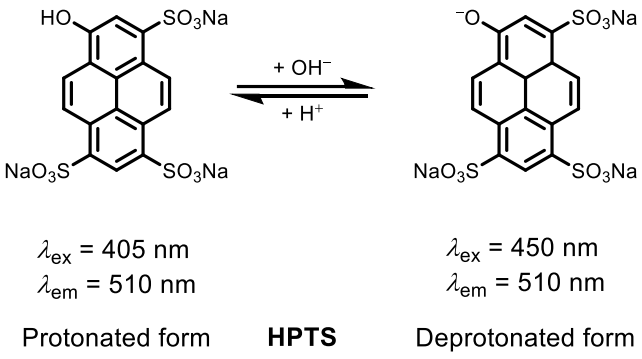

Figure 3: Protonated and deprotonated form of HPTS dye.

In a clean and well-dried fluorescence cuvette, 1975 µL of HEPES buffer which contained 10 mM HEPES, 100 mM NaCl, pH = 7.0, 25 µL of EYPC–LUVs⊃HPTS vesicles and magnetic bead was taken. The cuvette was placed under slow stirring using a magnetic stirrer integrated with the fluorescence instrument (t = 0 s). Time dependent HPTS emission intensity was monitored at λ_{em} = 510 nm (λ_{ex} = 450 nm). A pH gradient (~0.8) between the intra- and extra-vesicular systems was created by adding 20 µL of NaOH (0.5 M) at t = 20 s. By varying the concentrations of channel-forming molecules in DMSO were then introduced at t = 100 s. Finally, the vesicles were lysed by adding 25 µL of 10% Triton X-100 solution at t = 300 s to eliminate the pH gradient (Figure 4). The time axis was normalized according to Equation 1 :

$$t = t - 100 \qquad \text{Equation 1}$$

where, in normalized data t = 0 s was the timing of compound addition during the experiment, and t = 200 s was the timing of Triton X–100 addition.

The time-dependent data were normalized to fractional fluorescence intensity (in percentage) by using Equation 2

$$I_F = \left(\frac{I_t - I_0}{I_\infty - I_0}\right) \times 100 \qquad \text{Equation 2}$$

where, I_0 = Fluorescence intensity at t = 0 s, I_∞ = Final fluorescence intensity after addition of Triton X–100, I_t = Fluorescence intensity at time t.

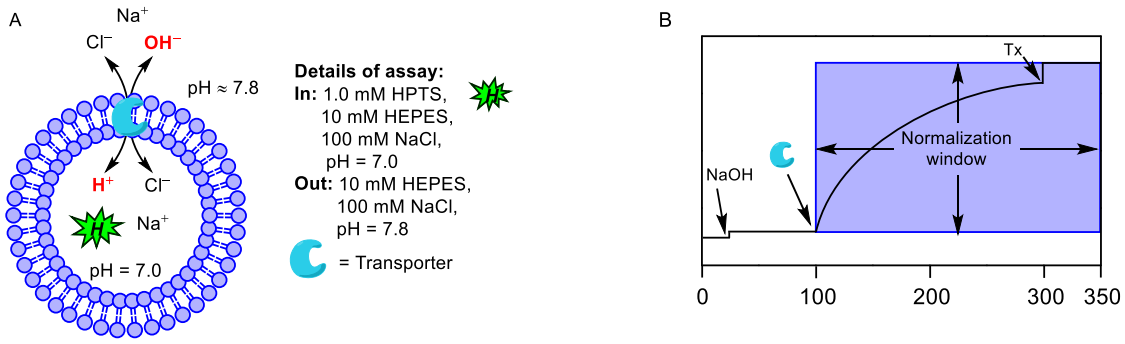

Figure 4: Schematic illustration of ion transport activity across EYPC–LUVs⊃HPTS vesicle (A), and the normalization framework for the fluorescence kinetics experiment of ion transport (B).

<u>Comparison of ion transport activity in EYPC–LUVs⊃HPTS</u>: To investigate the relative transport activity of channel-forming molecules **1a**-**1d,** an experiment of ion

transport was performed across the EYPC–LUVs⊃HPTS. A comparative study with 0.9 μM concentration revealed the activity sequence of **1c** > **1d** >>**1b**>**1a** (Figure 5).

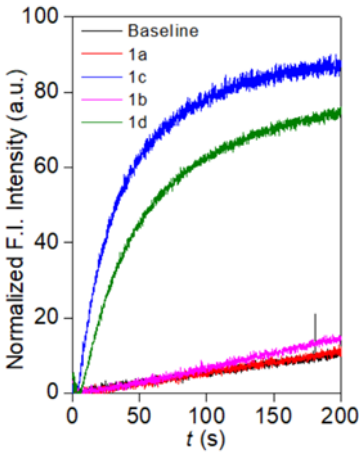

Figure 5: Comparative study of compound **1a**–**1d** at 0.9 μM with NaCl salt across EYPC–LUVs⊃HPTS

Dose-response activity in EYPC–LUVs⊃HPTS: We analyzed the fluorescence kinetics of each channel-forming molecule at varying concentrations over time. To determine the effective concentration (EC_{50}), the concentration profile must be assessed at $t = 190$ s. The EC_{50}, which represents the concentration of the transporter required to achieve 50% ion efflux activity, is calculated using the Hill equation (i.e. Equation 3):

$$Y = Y_{\infty} + \frac{(Y_0 - y_{\infty})}{[1+(c/EC_{50})^n]} \qquad \text{Equation 3}$$

In this equation, Y_0 refers to the fluorescence intensity measured just before the addition of the channel-forming molecule (at $t = 0$ s), while Y_∞ represents the fluorescence intensity observed at an excess compound concentration. The variable c denotes the concentration of the channel-forming molecule, and n, the Hill coefficient, indicates the number of monomers required to assemble into an active supramolecule.

Dose-response activity of compounds 1a-1d with NaCl salt:

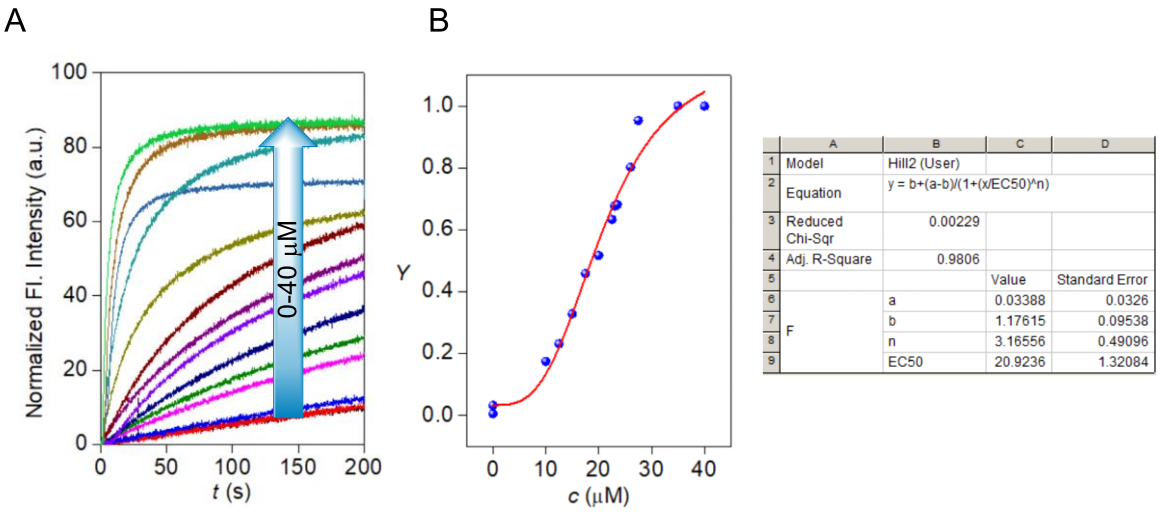

	A	B	C	D
1	Model	Hill2 (User)		
2	Equation	y = b+(a-b)/(1+(x/EC50)^n)		
3	Reduced Chi-Sqr	0.00229		
4	Adj. R-Square	0.9806		
5			Value	Standard Error
6	F	a	0.03388	0.0326
7		b	1.17615	0.09538
8		n	3.16556	0.49096
9		EC50	20.9236	1.32084

Figure 6: Dose-response activity of compound **1a** (0-40 µM) with NaCl salt across EYPC–LUVs⊃HPTS (A), and corresponding Hill plot of compound **1a** at *t* = 190 s (B).

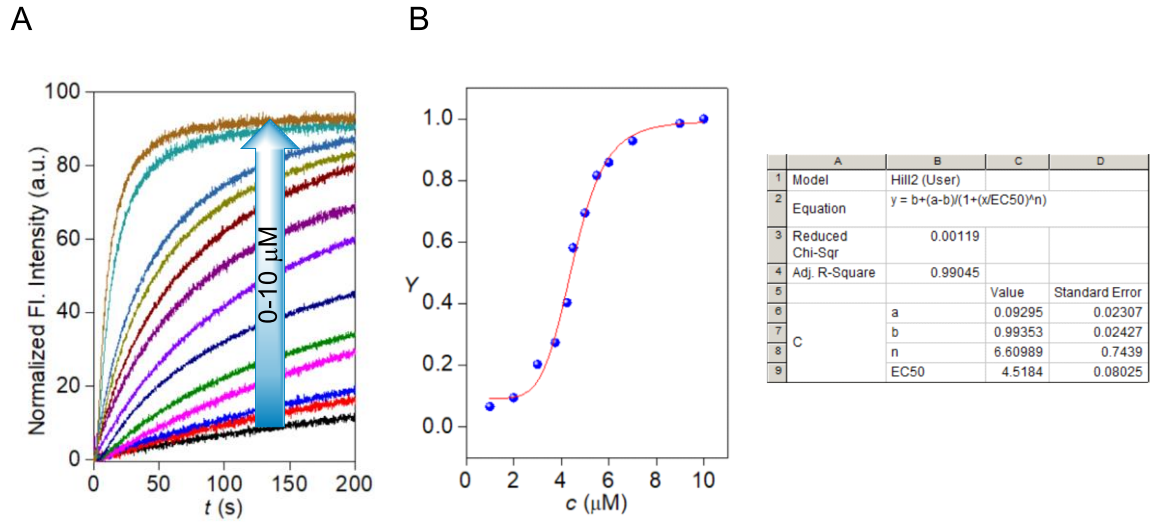

	A	B	C	D
1	Model	Hill2 (User)		
2	Equation	y = b+(a-b)/(1+(x/EC50)^n)		
3	Reduced Chi-Sqr	0.00119		
4	Adj. R-Square	0.99045		
5			Value	Standard Error
6	C	a	0.09295	0.02307
7		b	0.99353	0.02427
8		n	6.60989	0.7439
9		EC50	4.5184	0.08025

Figure 7: Dose-response activity of compound **1b** (0-10 µM) with NaCl salt across EYPC–LUVs⊃HPTS (A), and corresponding Hill plot of compound **1b** at *t* = 190 s (B).

A B

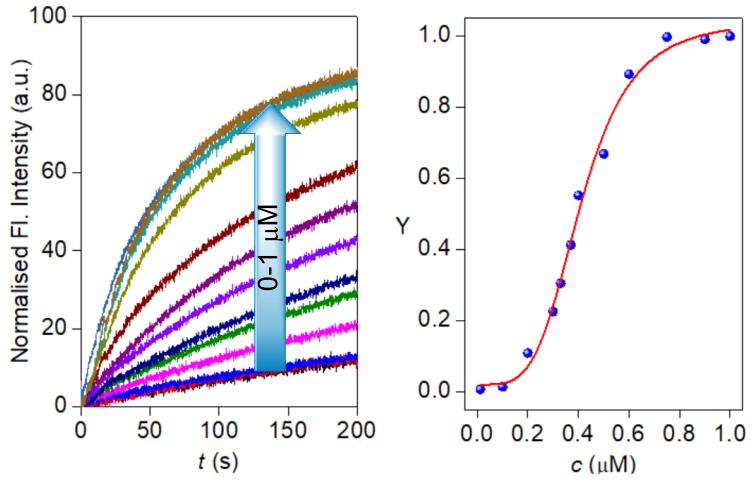

	A	B	C	D
1	Model	Hill2 (User)		
2	Equation	y = b+(a-b)/(1+(x/EC50)^n)		
3	Reduced Chi-Sqr	0.0013		
4	Adj. R-Square	0.99145		
5			Value	Standard Error
6	D	a	0.02018	0.02371
7		b	1.04478	0.03417
8		n	4.07822	0.47258
9		EC50	0.41145	0.01227

Figure 8 Dose-response activity of compound **1c** (0-1 µM) with NaCl salt across EYPC–LUVs⊃HPTS (A), and corresponding Hill plot of compound **1c** at *t* = 190 s (B).

A B

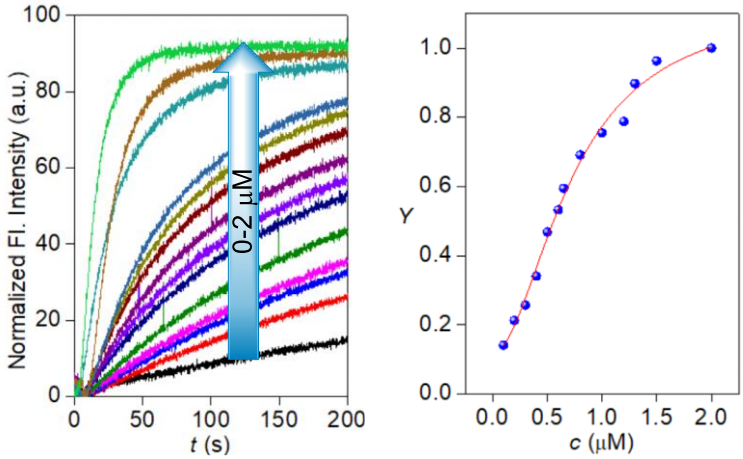

	A	B	C	D
1	Model	Hill2 (User)		
2	Equation	y = b+(a-b)/(1+(x/EC50)^n)		
3	Reduced Chi-Sqr	9.03398E-4		
4	Adj. R-Square	0.98931		
5			Value	Standard Error
6	D	a	0.11599	0.0368
7		b	1.13449	0.08372
8		n	1.89107	0.3046
9		EC50	0.72748	0.06641

Figure 9: Dose-response activity of compound **1d** (0-1 µM) with NaCl salt across EYPC–LUVs⊃HPTS (A), and corresponding Hill plot of compound **1d** at *t* = 190 s (B).

The Hill graph was plotted based on the dose-response studies of compounds **1a**, **1b**, **1c**, **1d** (Figures 6-9). The EC_{50} values were calculated using Equation 3, resulting in 20.9236 uM for **1a**, 4.5184 uM for **1b**, 0.41145 uM for **1c**, 0.72748 uM for **1d**. These results indicate that the activity sequence across EYPC–LUVs⊃HPTS is **1c** > **1d** > **1b** > **1a**.

4.2.2. Studies of ion selectivity across EYPC–LUVs⊃HPTS:

Preparation of Buffer and Stock solution: HEPES buffer was prepared by dissolving an appropriate amount of solid HEPES and a salt (either of NaF, NaCl, NaOAc, NaSCN, LiCl, KCl, RbCl, and CsCl) in autoclaved water to get 10 mM HEPES and 100 mM salt respectively. Subsequently, the pH was adjusted to 7.0 by the addition of 0.5 M NaOH solution. The stock solution of most active compound **1c** was prepared in HPLC grade DMSO solution for the studies.

Cation selectivity assay: A clean fluorescence cuvette was prepared, and 1975 µL of HEPES buffer which contained 10 mM HEPES, 100 mM MCl, at pH = 7.0: where M^+ = Li^+, Na^+, K^+, Rb^+, and Cs^+ were introduced. Following this, 25 µL of earlier prepared vesicle (EYPC–LUVs⊃HPTS) was carefully added under slow stirring (900 rpm) using magnetic stirrer equipped with a fluorescence instrument at t = 0 s. The emission intensity of HPTS at λ_{em} = 510 nm and (λ_{ex} = 450 nm) was continuously monitored over time. To establish a pH gradient (~0.8) between intra and extravesicular environment, 20 µL of 0.5 M NaOH was introduced at t = 20 s. At t = 100 s, the channel forming molecule **1c** was incorporated, and at t = 300 s, 25 µL of 10% Triton X–100 was added to completely lyze the vesicles, ensuring the full dissipation of the pH gradient.

For data analysis and comparison, normalization of time (X-axis) was performed using Equation 1, where the point of addition of the channel-forming molecule i.e. previously at t = 100 s was set to t = 0 s, and the experiment endpoint which was previously at t = 300 s was adjusted to t = 200 s. The fluorescence intensities (I_t) were converted into fractional emission intensity (I_F) using equation 2.

The fluorescence spectrum of compound **1c** with MCl salts (i.e. different cations) is shown in Figure 10. From the graph it, it can be concluded that no cationic binding site is present in our synthetic transporter, which means the data indicate that the cation does not participate in ion transport movement.

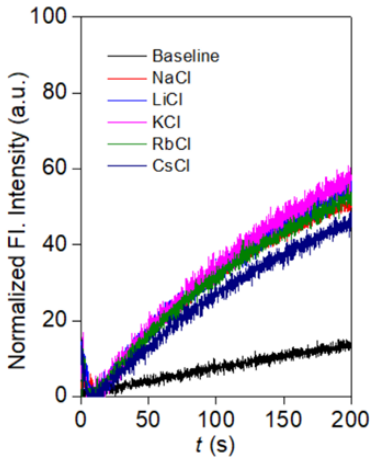

Figure 10: Cation selectivity of **1c** with different salts across EYPC-LUVs⊃HPTS at 500 nM concentration.

Anion selectivity assay: A clean fluorescence cuvette was prepared by adding 1975 µL of HEPES buffer which contained 10 mM HEPES, 100 mM NaX, pH = 7.0; where, X^- = F^-, Cl^-, OAc^-, and SCN^-, then 25 µL earlier prepared vesicle (EYPC–LUVs⊃HPTS) were added to the cuvette. The magnetic bead was taken. Next, the cuvette was placed under slow stirring conditions (900 rpm) using a magnetic stirrer integrated with the fluorescence instrument, and the experiment commenced at t = 0 s. Over time, the fluorescence intensity of HPTS dye was monitored at an emission wavelength of 510 nm (λ_{ex} = 450 nm). At t = 20 s, a pH gradient was established by adding 20 µL of 0.5 M NaOH. Subsequently, at t = 100 s, the channel-forming molecule **1c** was introduced. Later, 25 µL of 10% Triton X-100 was added at t = 300 s, to disrupt all vesicles, thereby eliminating the pH gradient.

To analyze the data, time (X-axis) was normalized using equation 1, where the addition of the channel-forming molecule at t = 100 s was set as t = 0 s, and the experiment's endpoint at t = 300 s was adjusted to t = 200 s. Fluorescence intensities (I_t) were converted into fractional emission intensity (I_F) using Equation 2.

The fluorescence graph (Figure 11) illustrates the transport activity of compound **1c** in the presence of NaX salts containing different anions. From the graph, it can be inferred that the synthetic ion transporters possess anion-binding sites, with the transport rate following the sequence Cl^-, F^-, OAc^-, SCN^-. This finding suggests that the synthetic ion transporter **1c** exhibits a high selectivity for chloride anions over other anions.

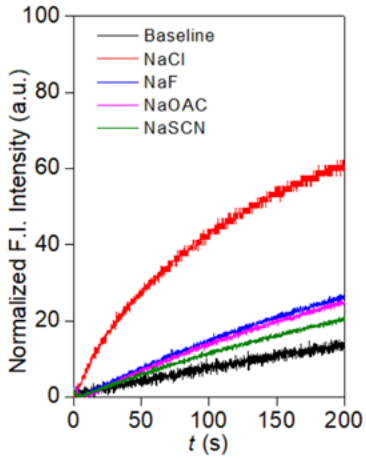

Figure 11: Anion selectivity of **1c** with different anions across EYPC-LUVs⊃HPTS at 500 nM concentration.

4.2.3. Chloride transport activity across EYPC–LUVs⊃lucigenin vesicles:

Preparation of buffer and stock solution: To prepare the HEPES buffer, an appropriate amount of solid HEPES and $NaNO_3$ salt was dissolved in autoclaved water to obtain final concentrations of 10 mM HEPES and 200 mM $NANO_3$, respectively. Then, 0.5 M NaOH solution was added to adjust the pH to 7.0. For the studies, the stock solution of the most active compound **1c** was prepared by dissolving it in HPLC-grade CH_3CN solution.

Preparation of EYPC–LUVs⊃lucigenin: In a clean and dry round bottom flask (10 mL), 1 mL of EYPC (25 mg/mL stock in $CHCl_3$) was added. The solution was dried by purging nitrogen with continuous rotation to form a thin transparent film. The transparent thin film was kept under a high vacuum for 4 h to remove excess $CHCl_3$ at room temperature. The resulting film was hydrated with 1 mL of buffer containing 1 mM lucigenin, 10 mM HEPES, 200 mM $NaNO_3$, and pH=7.0, and the resulting suspension was vortexed at 10 min intervals for 1 h. After that the resulting suspension was subjected to freeze-thaw (liquid nitrogen) for 23 cycles followed by extrusion through 200 nm pore size containing polycarbonate membrane for 23 times (must be an odd number) in order to get the vesicles of average diameter of 200 nm. Extravesicular dyes were removed by gel filtration using Sephadex G-50 with earlier prepared buffer solution (10 mM HEPES, 200 mM $NaNO_3$, pH=7.0) and further diluted to 4 mL to get desired EYPC–LUVs⊃lucigenin vesicles. Final conditions: ~ 5 mM

EYPC, Inside: 1 mM lucigenin, 10 mM HEPES, 200 mM $NaNO_3$, pH = 7.0; Outside: 10 mM HEPES, 200 mM $NaNO_3$, pH = 7.0.

Cation selectivity across EYPC–LUVs⊃lucigenin: Lucigenin is a chloride-sensitive dye. Due to the charge transfer process, its fluorescence emission is quenched upon exposure to chloride ions.[19] A clean fluorescence cuvette was prepared by taking 1975 µL of buffer solution which contained 10 mM HEPES, 200 mM $NaNO_3$, pH = 7.0. Followed by 25 µL of EUPC–LUVs⊃lucigenin, and a magnetic bead was added. The solution was then placed under stirring conditions (900 rpm) using fluorescence instrument equipped with a magnetic stirrer, initiating the experiment at t = 0 s. Over time, the fluorescence intensity of lucigenin was monitored at an emission wavelength of 535 nm (λ_{ex} = 455 nm). At t = 20 s, a chloride gradient was established in the extravesicular environment by adding 33.3 µL of 2.0 M chloride salts containing different cations, where; M^+ = Li^+, K^+, Na^+, Rb^+, Cs^+. Then, at t = 100 s, the channel-forming compound **1c** was introduced on solution. Finally, 25 µL of 10% Triton X-100 was added at t = 300 s, leading to vesicle destruction. As a result, the lucigenin became exposed to higher concentration of chloride ions in the extravesicular surroundings, causing fluorescence quenching.

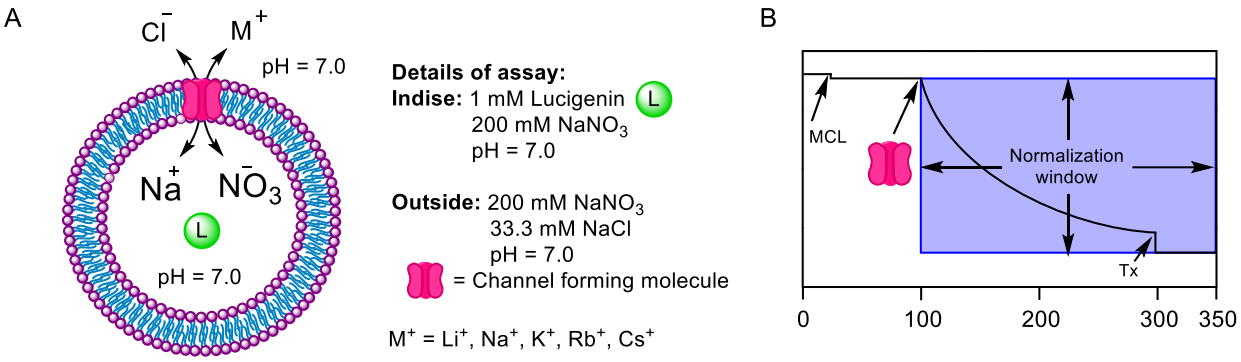

Figure 12: Schematic representation of ion transport activity across EYPC–LUVs⊃lucigenin vesicle (A) and normalization framework for the fluorescence kinetics experiment of ion transport (B).

The time axis (X-axis) was normalized by using Equation 4:

$$t = t - 100 \qquad \text{Equation 4}$$

where, in normalized data t = 0 s was the timing of compound addition during the experiment, and t = 200 s was the timing of Triton X–100 addition.

The time-dependent data were normalized to fractional fluorescence intensity (in percentage) using Equation 5

$$Y = Y_{\infty} + \frac{(Y_0 - y_{\infty})}{[1+(c/EC_{50})^n]} \qquad \text{Equation 5}$$

where, I_0 = Fluorescence intensity just before the channel forming molecule addition (at 0 s), I_∞ = Final fluorescence intensity after addition of Triton X–100, I_t = Fluorescence intensity at time *t*. The fluorescence spectrum of compound **1c** with MCl salts (i.e. K^+, Li^+, Na^+, Rb^+, Cs^+) shows in Figure 13. From the graph we can conclude that our transporters does not selective towards metal ions.

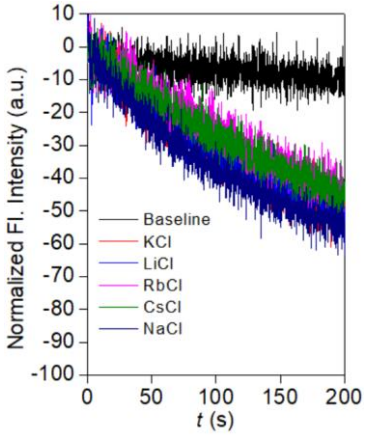

Figure 13: Cation selectivity of compound **1c** (2.5 μM) by varying the extravesicular cations.

4.2.4. Mechanistic study of ion transport across EYPC–LUVs⊃lucigenin:

Chloride transport by lucigenin assay in presence of valinomycin: Valinomycin functions primarily as a potassium (K^+) uniporter, particularly in environments with strongly hydrated anions such as chloride (Cl^-), where ion pairing is less favourable. Its transport mechanism is passive, selective, and electrogenic, consistent with the characteristics of a uniporter. A clean fluorescence cuvette was prepared by taking 1975 μL of buffer solution which contained 10 mM HEPES, 200 mM $NaNO_3$, pH = 7.0. Followed by 25 μL of EUPC–LUVs⊃lucigenin, and a magnetic bead was added. The solution was then placed under stirring conditions (900 rpm) using fluorescence instrument equipped with a magnetic stirrer, initiating the experiment at *t* = 0 s. Over time, the fluorescence intensity of lucigenin was monitored at an emission wavelength of 535 nm (λ_{ex} = 455 nm). At *t* = 20 s, a chloride gradient was established in the extravesicular environment by adding 33.3 μL of 2.0 M KCl. Then, at *t* = 100 s, the

channel-forming compound **1c** was introduced into the solution. Finally, at *t* = 300 s, 25 µL of 10% Triton X-100 was added, leading to vesicle destruction. As a result, the lucigenin became exposed to a higher concentration of chloride ions in the extravesicular surroundings, causing fluorescence quenching. This time-dependent data was subsequently normalized using Equation 4. From the fluorescent graph (Figure 15), we can infer that our transporter has transported the ions via the antiport mechanism.

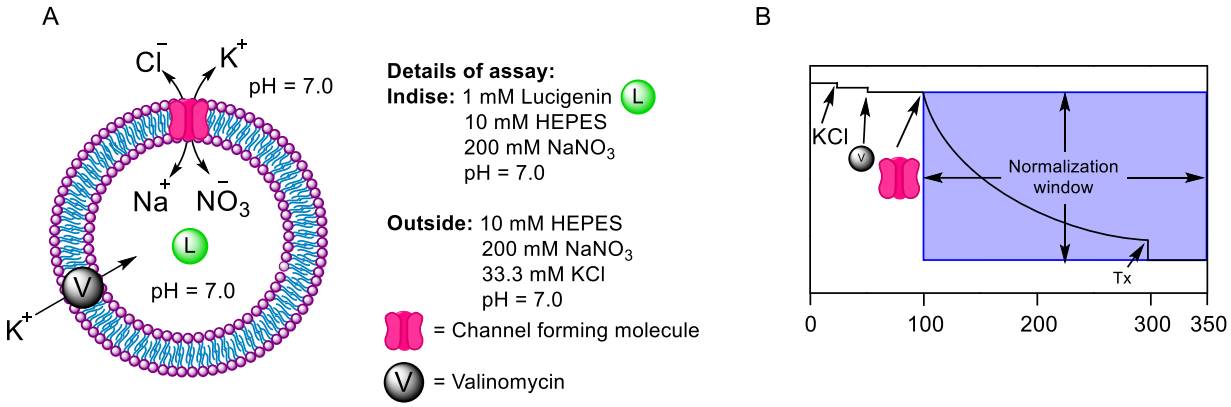

Figure 14: Schematic illustration of valinomycin assay across EYPC–LUVs⊃lucigenin with KCl salt (A), and the normalization framework for the fluorescence kinetics experiment of ion transport (B).

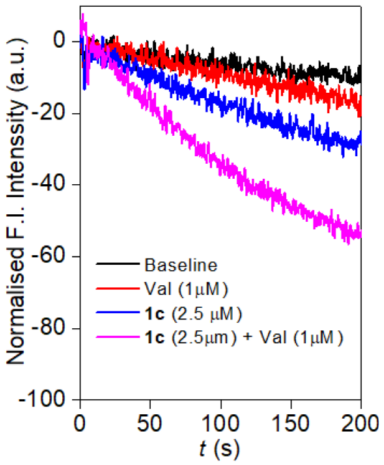

Figure 15: Chloride influx by compound **1c** in the presence and absence of valinomycin across EYPC–LUVs⊃lucigenin with KCl salt.

4.2.5. Calcein leakage assay:

EYPC–LUVs were loaded with the self-quenching dye calcein at a concentration of 50 mM. Calcein exhibits self-fluorescence quenching at high concentrations, but its efflux

through pores formed by compound **1c** results in an increase in fluorescence emission intensity. For the assay, two distinct buffer solutions were prepared: Buffer A, consisting of 10 mM HEPES at pH = 7.0, and Buffer B, which included 10 mM HEPES and 150 mM NaCl at pH 7.0.

Preparation of EYPC–LUVs⊃Calcein: In a clean and dry 10 mL round-bottom flask, 0.5 mL of EYPC (25 mg/mL stock in $CHCl_3$) was taken. To form a thin transparent film, the solution was dried by purging nitrogen while continuously rotating the flask. The film was then placed under high vacuum at room temperature for 4 hours to remove excess $CHCl_3$. Next, the resulting film was hydrated with 0.5 mL of buffer containing 10 mM HEPES, pH = 7.0, and the obtained suspension was vortexed at 10-minute intervals for 1 hour. Following this, the suspension underwent 23 times freeze-thaw cycles using liquid nitrogen, after which it was extruded 23 times (ensuring an odd number) through a polycarbonate membrane with 200 nm pore size to obtain vesicles with an average diameter of 200 nm. To remove extravesicular dyes, gel filtration was performed using Sephadex G-50 with a previously prepared buffer A solution (10 mM HEPES, pH = 7.0). Finally, the solution was diluted to 3 mL to obtain EYPC–LUVs⊃Calcein.

Calcein assay: A clean fluorescence cuvette was prepared by adding 1975 µL of buffer solution B which contained 10 mM HEPES, 150 mM NaCl, pH =7.0. Then, 25 µL of EYPC–LUVs⊃Calcein and magnetic bead was added. The solution was then placed under stirring conditions (900 rpm) using a fluorescence instrument equipped with a magnetic stirrer, and the experiment was initiated at t = 0 s. Over time, the fluorescence intensity of calcein was monitored at an emission wavelength of 520 nm (λ_{ex} = 490 nm). At t = 1 min 40 sec, the channel-forming compound **1c** was introduced at varying concentrations. Finally, at t = 5 min, 25 µL of Triton X-100 was added, leading to vesicle destruction and the subsequent efflux of calcein dye. The time-dependent fluorescence data were then normalized to fluorescence intensity in percentage using Equation 2, while the time axis was adjusted using Equation 1.

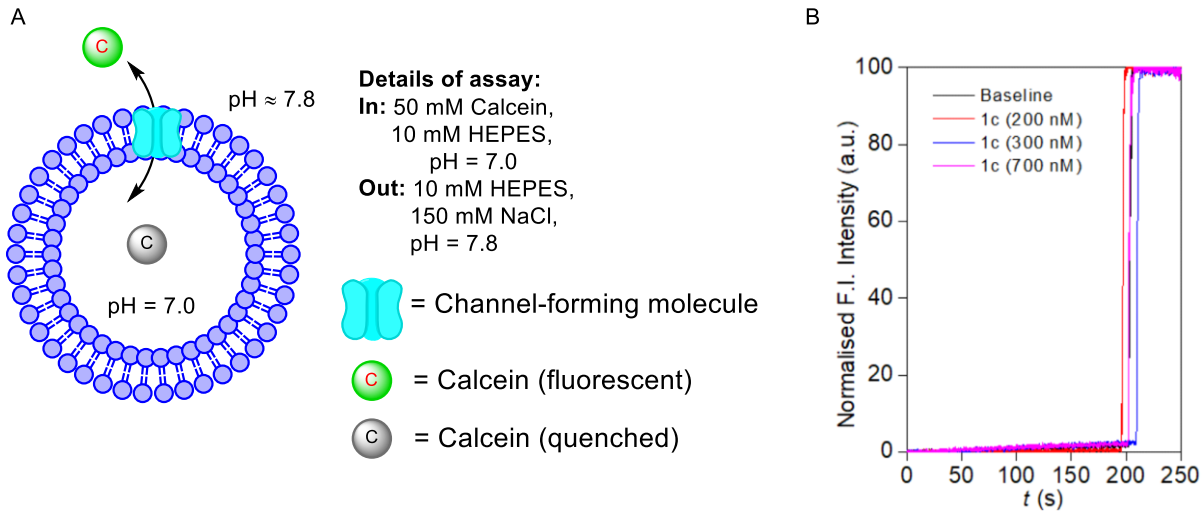

Figure 16: Schematic illustration of calcein assay across EYPC–LUVs⊃Calcein (A), fluorescence kinetics of compound **1c** across EYPC–LUVs⊃Calcein at different concentration (B).

4.2.6. Single Crystal X-Ray Diffraction Study:

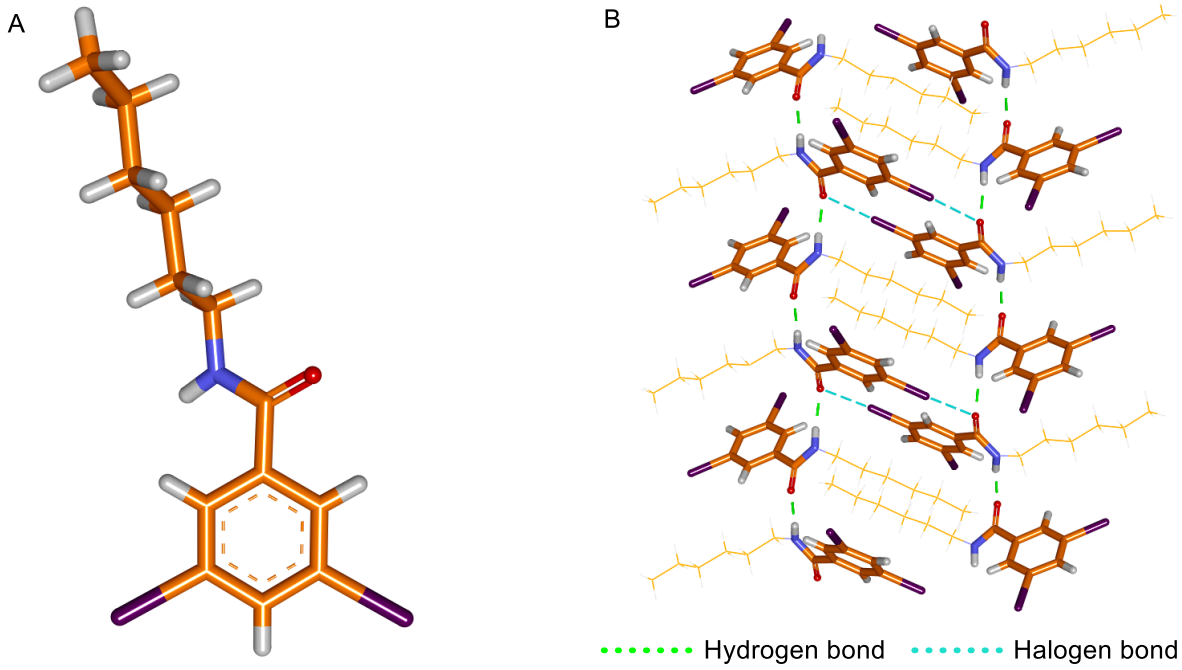

Figure 17: Crystal structure of compound **1c** (A) and the corresponding self-assembled crystal structure with hydrogen and halogen bonding (B).

The compound **1c** was crystalised crystallized as a yellow solid by slow evaporation of chloroform and methanol solvent, respectively, to get a single crystal appropriate for X–ray examination. The single crystal data were obtained on a Bruker Smart Apex Duo diffractometer using Mo Kα radiation (λ = 0.71073 Å) for compound **1c** at 296 K.

The crystal structure revealed that the molecular configuration within the crystalline lattice exhibits the anti-parallel orientation where the 3,5-diiodobenzene ring of one molecule is just above the alkyl chain (n-hexane) of the next molecule. This arrangement creates the ABAB pattern in self-assembly. The intermolecular hydrogen bonding between the C=O---NH carbonyl group and amide group of other molecule has been observed and halogen bonding of carbonyl group and iodine group of other molecule i.e. C=O----I (Figure 17.B) also been observed.

5. NMR:

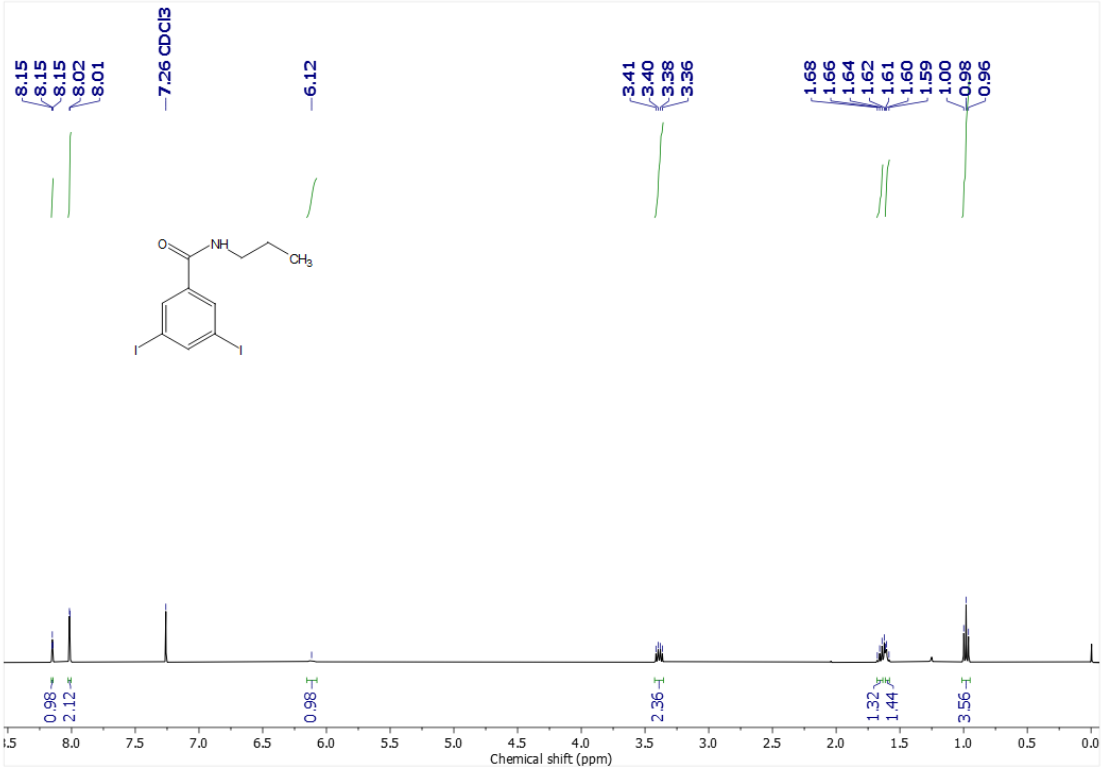

Figure 18: ^{1}H (400 MHz) NMR spectrum of compound **1a** in $CDCl_3$.

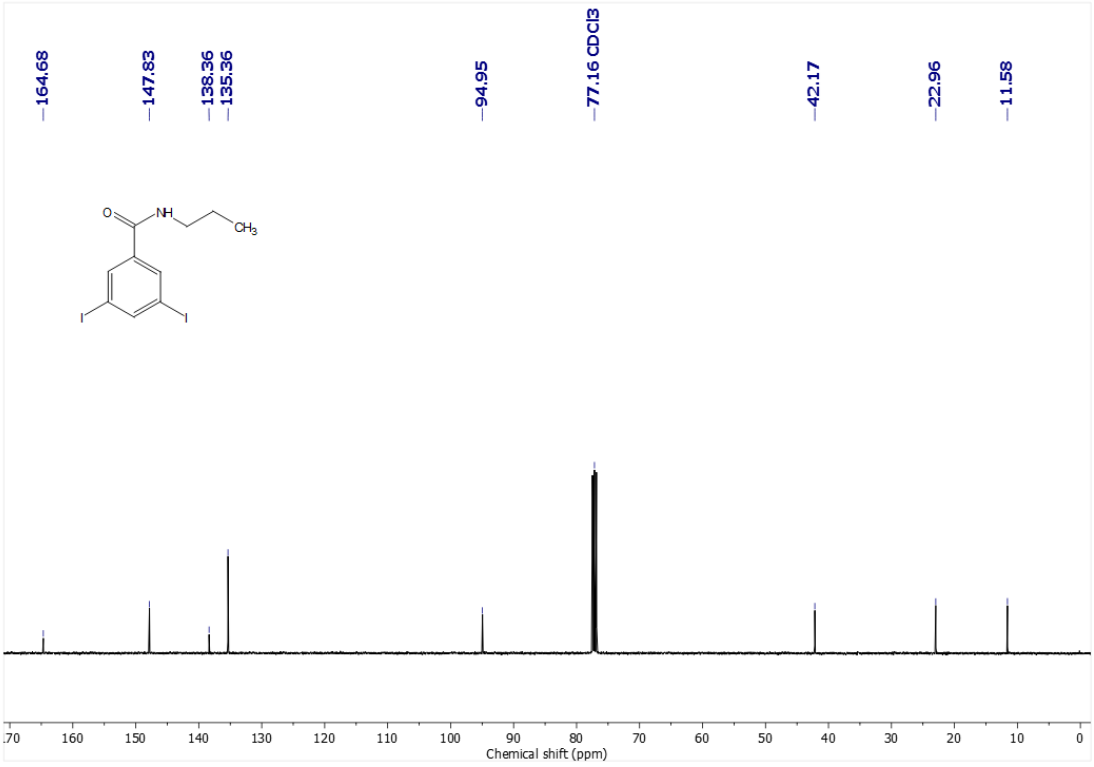

Figure 19: ^{13}C NMR (101 MHz) NMR spectrum of compound **1a** in $CDCl_3$.

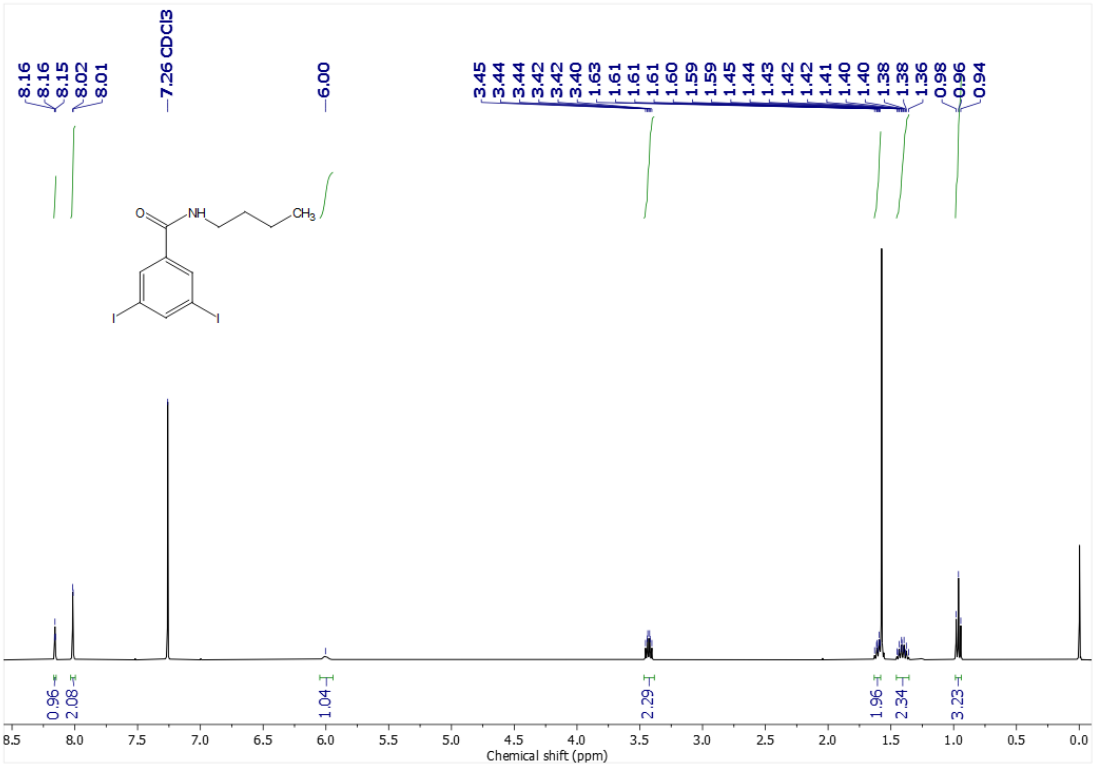

Figure 20: ^{1}H (400 MHz) NMR spectrum of compound **1b** in $CDCl_3$.

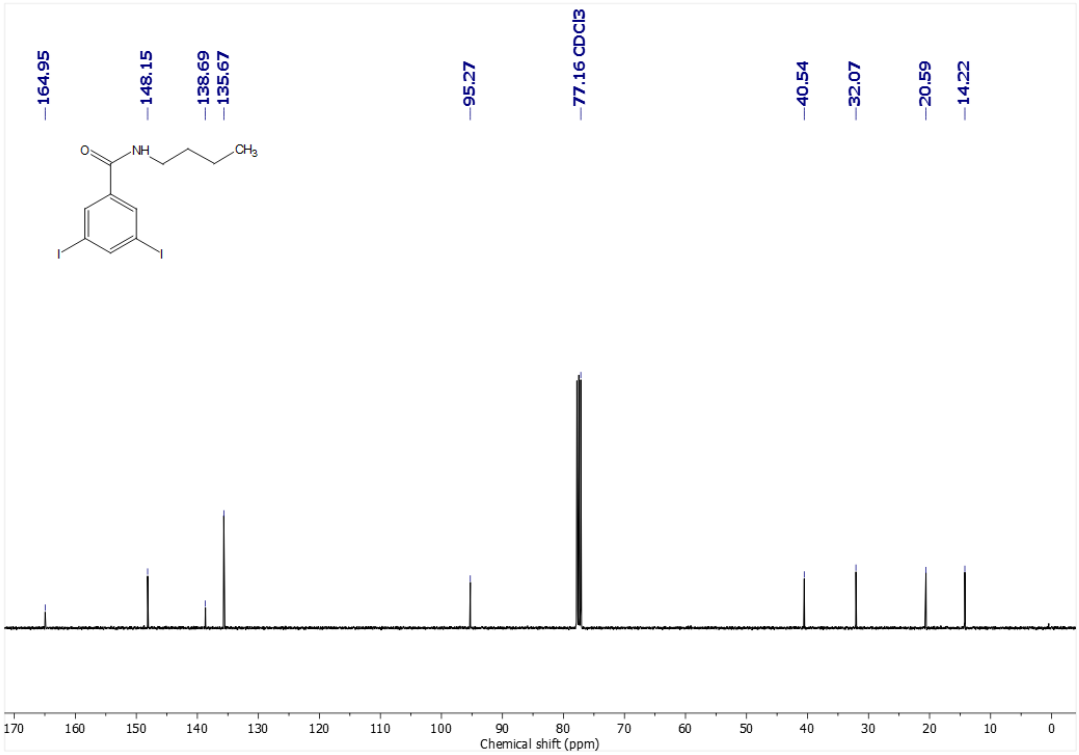

Figure 21: ^{13}C (101 MHz) NMR spectrum of compound **1b** in $CDCl_3$.

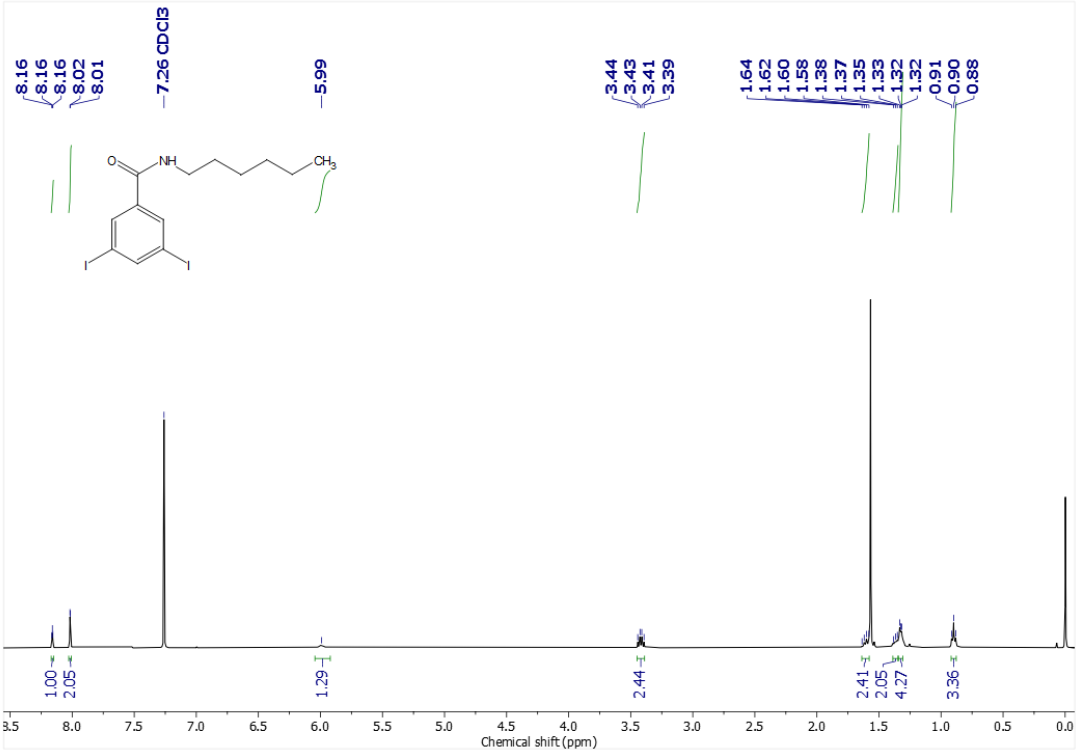

Figure 22: ^{1}H (400 MHz) NMR spectrum of compound **1c** in $CDCl_3$.

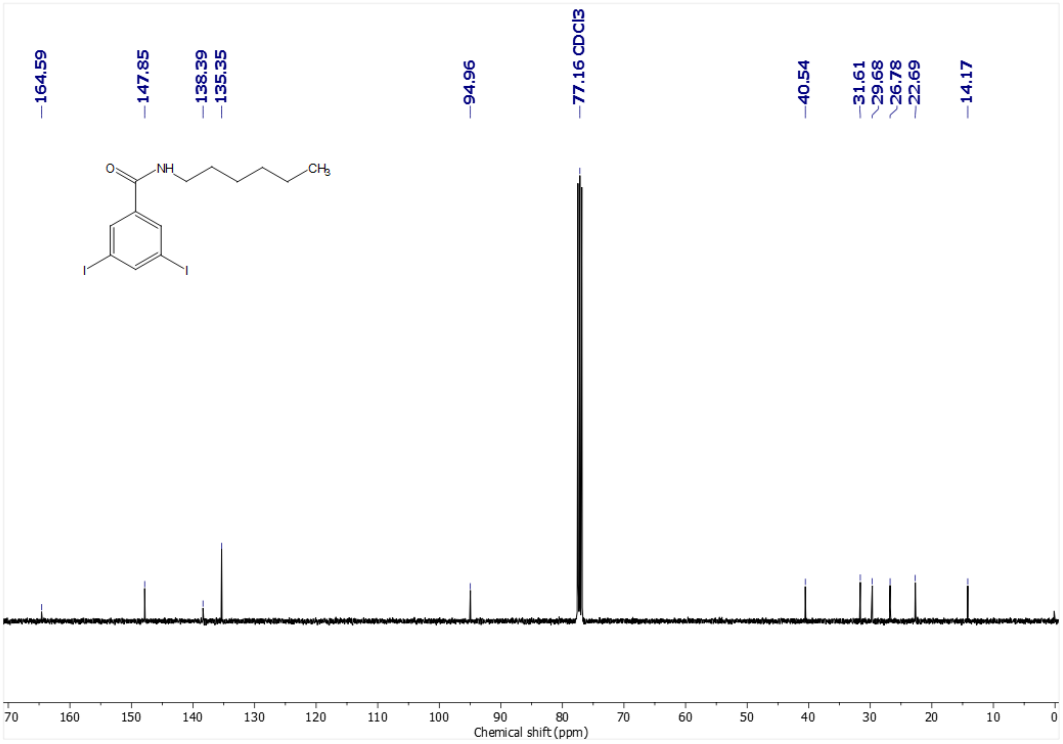

Figure 23: ^{13}C (101 MHz) NMR spectrum of compound **1c** in $CDCl_3$.

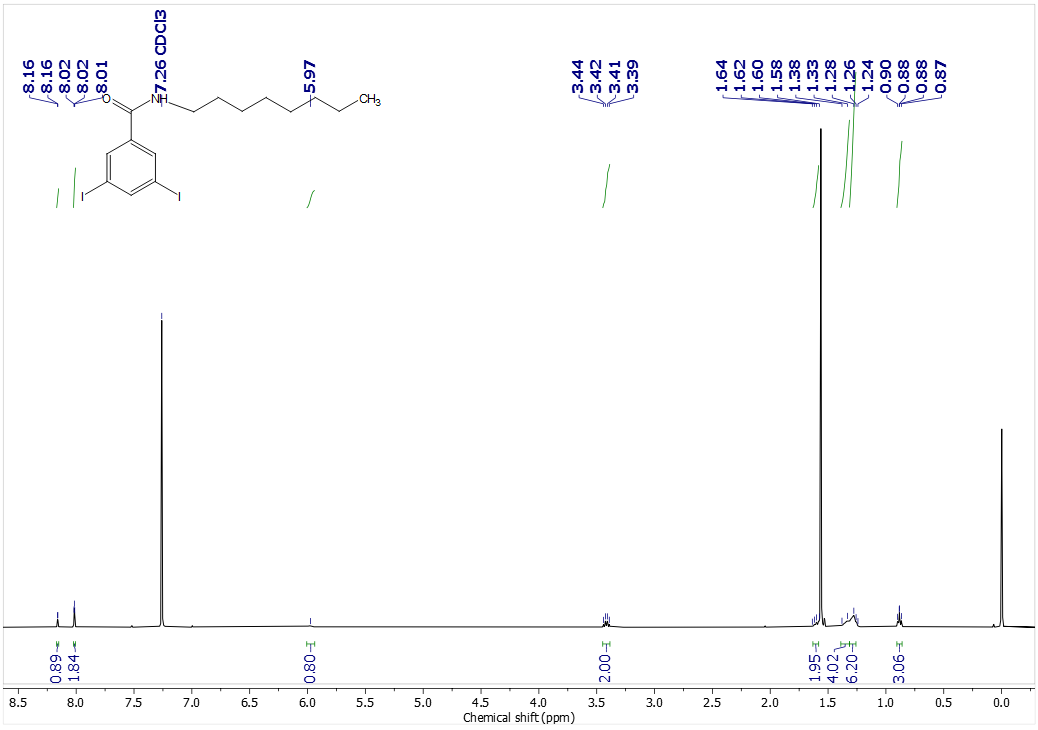

Figure 24: ^{1}H (400 MHz) NMR spectrum of compound **1d** in $CDCl_3$.

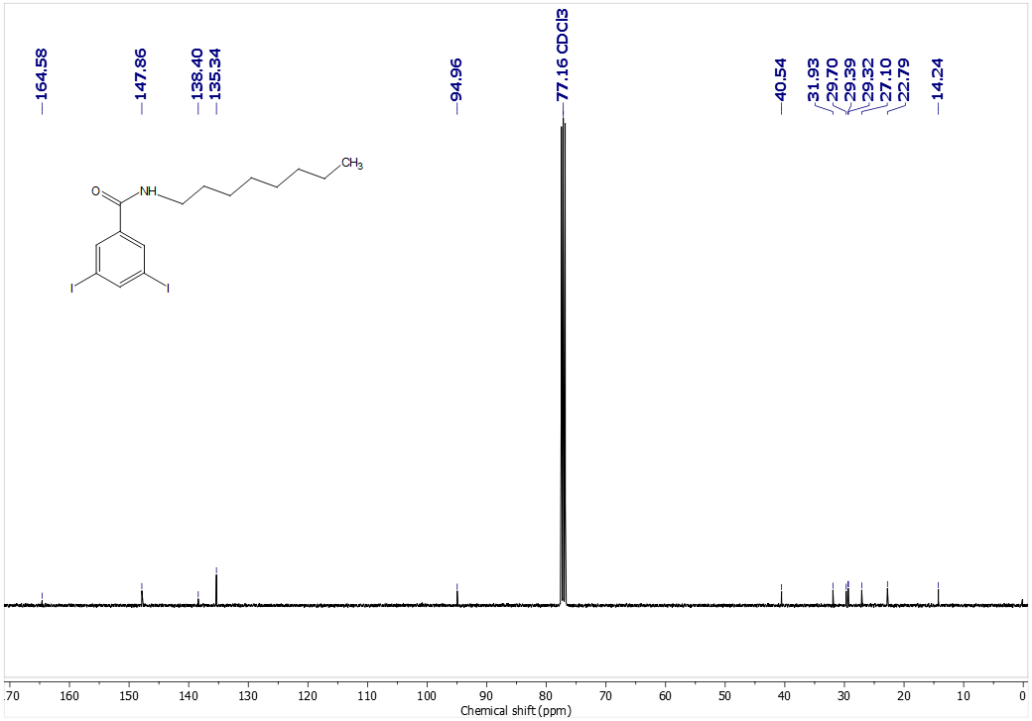

Figure 25: ^{13}C (101 MHz) NMR spectrum of compound **1d** in $CDCl_3$.

6. HRMS data:

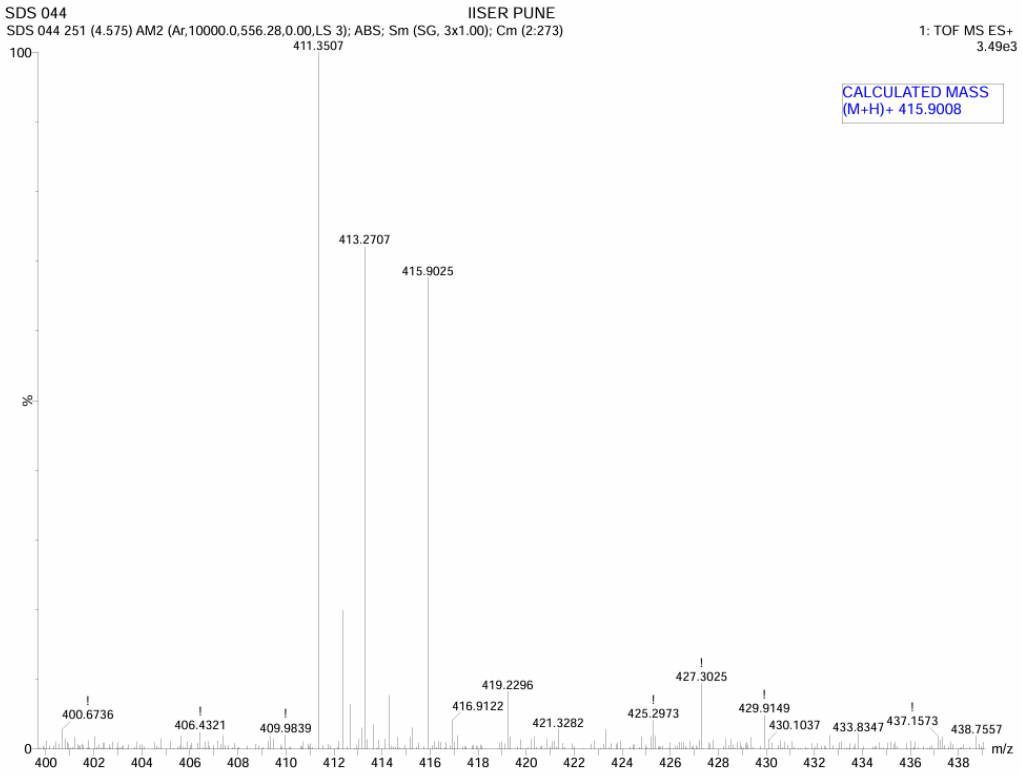

Figure 26: HRMS of compound **1a**.

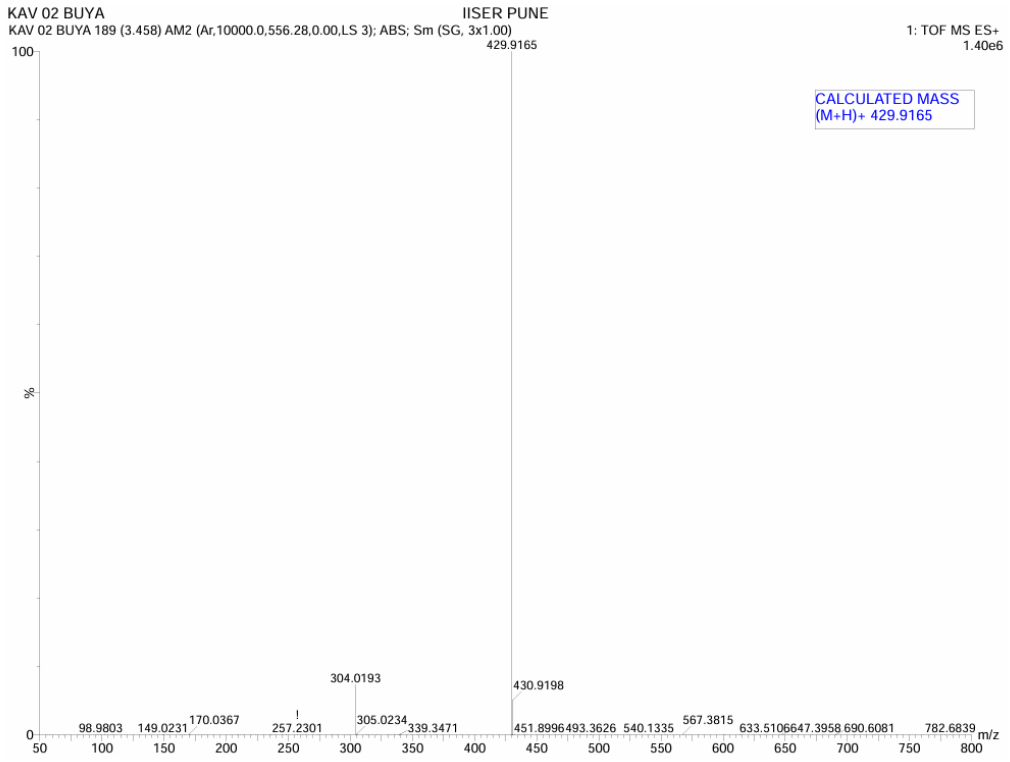

Figure 27: HRMS of compound **1b**.

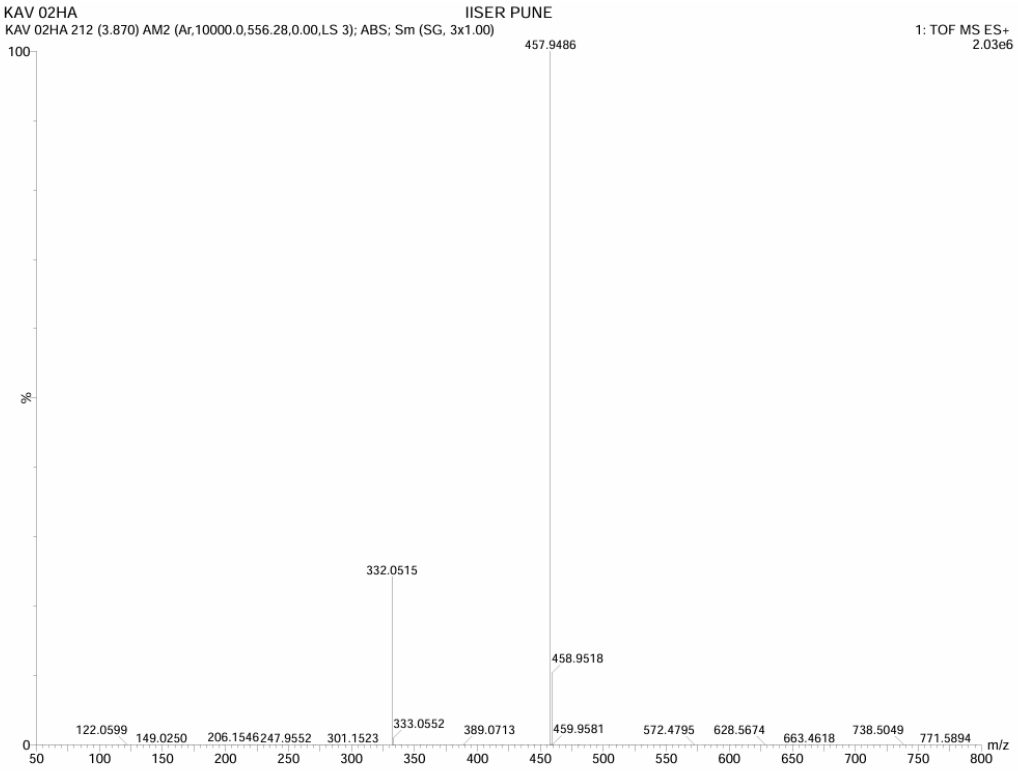

Figure 28: HRMS of compound **1c**.

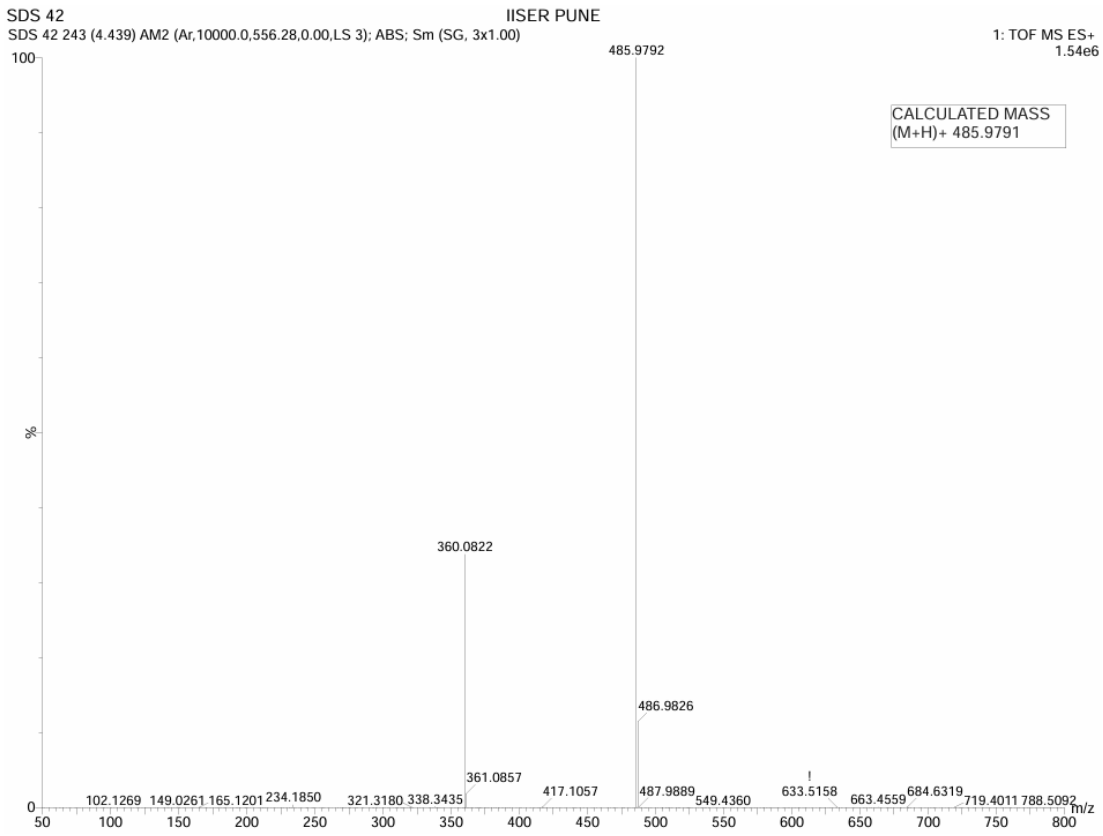

Figure 29: HRMS of compound **1d**.

7. Conclusion and future plan:

Among four synthesized derivatives of synthetic ion transporters, compound **1c** demonstrated the highest transport efficiency, evidenced by its lowest EC_{50} value in ion flux assays across lipid bilayers. **1c** exhibited selective transport for chloride ions, as confirmed by HPTS (8-hydroxypyrene-1,3,6-trisulfonic acid) fluorescence-based assays, with no observable selectivity for monovalent cations (Li^+, Na^+, K^+, Rb^+, and Cs^+). Mechanistic studies utilizing a valinomycin-mediated potassium gradient revealed that **1c** operates via an antiport mechanism. Calcein leakage assays further confirmed the absence of pore formation. Field-emission scanning electron microscopy (FESEM) analysis highlighted that **1c** has the capacity for remarkable self-assembly.

Currently, we are doing the concentration-dependent chloride influx study with our compound. In the future, we will also investigate the bilayer lipid membrane (BLM) experiments to prove the formation of the ion channel in the membrane.

8. References:

(1) Yan, T.; Liu, S.; Xu, J.; Sun, H.; Yu, S.; Liu, J. Unimolecular Helix-Based Transmembrane Nanochannel with a Smallest Luminal Cavity of 1 Å Expressing High Proton Selectivity and Transport Activity. *Nano Lett.* **2021**, *21* (24), 10462–10468.

(2) *Recommended Dietary Allowances: 10th Edition*; National Academies Press: Washington, D.C., 1989; p 1349.

(3) Duran, C.; Thompson, C. H.; Xiao, Q.; Hartzell, H. C. Chloride Channels: Often Enigmatic, Rarely Predictable. *Annu. Rev. Physiol.* **2010**, *72*, 95–121.

(4) Diamond, J. M.; Wright, E. M. Biological Membranes: The Physical Basis of Ion and Nonelectrolyte Selectivity. *Annu. Rev. Physiol.* **1969**, *31* (1), 581–646.

(5) Vaughan-Jones, R. D.; Spitzer, K. W.; Swietach, P. Intracellular pH Regulation in Heart. *J. Mol. Cell. Cardiol.* **2009**, *46* (3), 318–331.

(6) Jentsch, T. J.; Stein, V.; Weinreich, F.; Zdebik, A. A. Molecular Structure and Physiological Function of Chloride Channels. *Physiol. Rev.* **2002**, *82* (2), 503–568.

(7) Choi, J. Y.; Muallem, D.; Kiselyov, K.; Lee, M. G.; Thomas, P. J.; Muallem, S. Aberrant CFTR-Dependent HCO3- Transport in Mutations Associated with Cystic Fibrosis. *Nature* **2001**, *410* (6824), 94–97.

(8) Influence of Metal Ion Solutions on Rabbit Osteoclast Activities in Vitro. *Histol. Histopathol.* **2002**, No. 17, 1025–1032.

(9) Planells-Cases, R.; Jentsch, T. J. Chloride Channelopathies. *Biochim. Biophys. Acta* **2009**, *1792* (3), 173–189.

(10) Kotsias, B. A. Chapter 3 Basic Mechanisms of Ion Channel Function. In *Supplements to Clinical Neurophysiology*; Elsevier, 2002; Vol. 54, pp 33–42.

(11) Kass, R. S. The Channelopathies: Novel Insights into Molecular and Genetic Mechanisms of Human Disease. *J. Clin. Invest.* **2005**, *115* (8), 1986–1989.

(12) Verkman, A. S.; Galietta, L. J. V. Chloride Channels as Drug Targets. *Nat. Rev. Drug Discov.* **2009**, *8* (2), 153–171.

(13) Lam, A. K. M. Mechanism of Pore Opening in the Calcium-Activated Chloride Channel TMEM16A.

(14) Ashcroft, F. M. From Molecule to Malady. *Nature* **2006**, *440* (7083), 440–447.

(15) Li, S.; Moorefield, C. N.; Shreiner, C. D.; Wang, P.; Sarkar, R.; Newkome, G. R. A Rigid Metallohexameric Macrocycle Composed of Endo- and Exo-Cyclic Bisterpyridine-Metal Complexes. *New J. Chem.* **2011**, *35* (10), 2130.

(16) Chattopadhayay, S.; Banzal, K. V.; Talukdar, P. Photo-Activation of Tolane-Based Synthetic Ion Channel for Transmembrane Chloride Transport. *Angew. Chem. Int. Ed Engl.* **2025**, *64* (2), e202414354.

(17) Ahmad, M.; Roy, N. J.; Singh, A.; Mondal, D.; Mondal, A.; Vijayakanth, T.; Lahiri, M.; Talukdar, P. Photocontrolled Activation of Doubly *o* -Nitrobenzyl-Protected Small Molecule Benzimidazoles Leads to Cancer Cell Death. *Chem. Sci.* **2023**, *14* (33), 8897–8904.

(18) Malla, J. A.; Umesh, R. M.; Vijay, A.; Mukherjee, A.; Lahiri, M.; Talukdar, P. Apoptosis-Inducing Activity of a Fluorescent Barrel-Rosette M^+ /Cl^- Channel. *Chem. Sci.* **2020**, *11* (9), 2420–2428.

(19) Legg, K. D.; Hercules, D. M. Quenching of Lucigenin Fluorescence. *J. Phys. Chem.* **1970**, *74* (10), 2114–2118.